PHYSICAL REVIEW A VOLUME 36, NUMBER 11 DECEMBER 1, 1987

Dynamical singularities in ultradiffusion

W. P. Keirstead
Physics Department, Stanford University, Stanford, California 94305

B. A. Huberman
Xerox Corporation, Palo Alto Research Center, Palo Alto, California 94304
(Received 14 May 1987)

We study ultradiffusion in systems with an arbitrary distribution of energy barriers and nearest-neighbor hopping processes. As the effective temperature R is increased, we find power-law decay of the autocorrelation function with an anomalous R-dependent exponent for $R < R_c$. Furthermore, we observe singular crossover at R_c to normal diffusion. The value of R_c depends on the average branching ratio of the system. We have also discovered a set of trees for which the R dependence of the exponent departs from the expected value based on universality arguments. Analytical results and computer experiments for several systems are presented.

I. INTRODUCTION

Recently, there has been much interest in natural and artificial systems which possess an underlying hierarchical structure. Examples are provided, among others, by the structure of social organizations,[1] studies of relaxation phenomena in complex macromolecules,[2] and the decay of the remanent magnetization in spin glasses.[3] Common to all these systems is the existence of a multiplicity of time scales governing the relaxation process, leading to an overall rate of decay which in some cases can be much slower than exponential.

To model these phenomena, a number of authors have considered diffusive processes on simple hierarchical systems. The first model of this type, and the one which we study in this paper, was due to Huberman and Kerszberg (Ref. 4) (HK) and consists of a particle performing nearest-neighbor hopping over an ordered array of energy barriers in one dimension [see Fig. 1(a)]. It is assumed that the barrier heights are selected from a set $\{\varepsilon_0, \varepsilon_1, \ldots, \varepsilon_n, \ldots\}$, and that $\varepsilon_n = n\varepsilon_0$. As a result of this, one can see that there exists a unique tree structure corresponding to any configuration of barriers chosen from the above set [see Fig. 1(b) for the tree corresponding to the barriers in Fig. 1(a)]. In the tree picture, the hopping occurs at the leaves of the tree, and an ultrametric distance between a given pair of adjacent nodes can be defined to be the height of the energy barrier between them. It is the existence of such an underlying ultrametric structure that led HK to denote this diffusion process as "ultradiffusion."

Other authors have considered variants on the above problem. If one allows for long-range hopping then it is the transition rates themselves that form the ultrametric space.[5] Recently, Bachas and Huberman[6] have solved this problem exactly for an arbitrary arrangement of barriers and related the relaxation rate to the complexity of the tree itself. One can also consider the problem of a random walk on the tree itself, a model which has been proposed to account for the observed stickiness in the chaotic transport of particles.[7]

One of the primary drawbacks of the original HK analysis is that it considers only the ordered binary tree of Fig. 1(b). In this work we wish to investigate other arrangements of barriers corresponding to trees with no or only partial ordering. Although we find that many of the features exhibited by the binary tree carry over to the general case, we also discover certain properties that are not universal.

The organization of this paper is as follows. In Sec. II we review in some detail the basic results on the HK binary-tree model. In Sec. III we present an approximate solution for an ordered n-ary tree in one dimension. In Sec. IV we discuss the results of numerical simulations for a number of different systems. Section V presents a discussion of the results in higher-dimensionality systems, and Sec. VI summarizes the work and presents the main conclusions. The Appendix contains the details of the numerical methods used.

II. BASIC RESULTS

We consider a one-dimensional nearest-neighbor hopping problem in a thermally activated picture. In this case, the (symmetric) transition rate ω_n for hopping over barrier ε_n is given by

$$\omega_n = \exp(-\varepsilon_n/k_B T) = [\exp(-\varepsilon_0/k_B T)]^n \equiv R^n . \tag{2.1}$$

Here, R plays the role of a renormalized temperature. When $R=0$ (i.e., $T=0$), we have trapping; when $R=1$ (i.e., $T\to\infty$), all the transition rates are equal and we have normal diffusion.

If we let $P_n(t)$ denote the probability that the particle is in cell n at time t, then the master equation for the process is

$$\frac{dP_n}{dt} = \omega_{n,n+1}(P_{n+1} - P_n) + \omega_{n,n-1}(P_{n-1} - P_n) , \tag{2.2}$$

where $\omega_{n,k} = \omega_{k,n}$ is the transition rate between cells n

and k.

To investigate the diffusion process, one typically studies the autocorrelation function $P_0(t)$ or the mean-square displacement $d^2(t)$. $P_0(t)$ is defined to be the probability of the particle being in cell 0 at time t given that it was in cell 0 at $t=0$; it is averaged over all initial starting sites. Similarly, $d^2(t)$ is defined to be the mean-square distance traveled from the initial site, averaged over all initial sites. For normal diffusion (i.e., all transition rates equal), one can easily show that the long-time behaviors are $P_0(t)\approx t^{-1/2}$, and $d^2(t)\approx t^{+1}$. In the general case, we expect $P_0(t)$ to behave as $t^{-\nu}$ with an exponent ν which may depend on R and on the topology of the tree in question. One can show[8] for the same tree that $d^2(t)$ will behave as $t^{+2\nu}$. Thus to find the long-time behavior of the autocorrelation function, one can investigate the mean squared displacement, and vice versa.

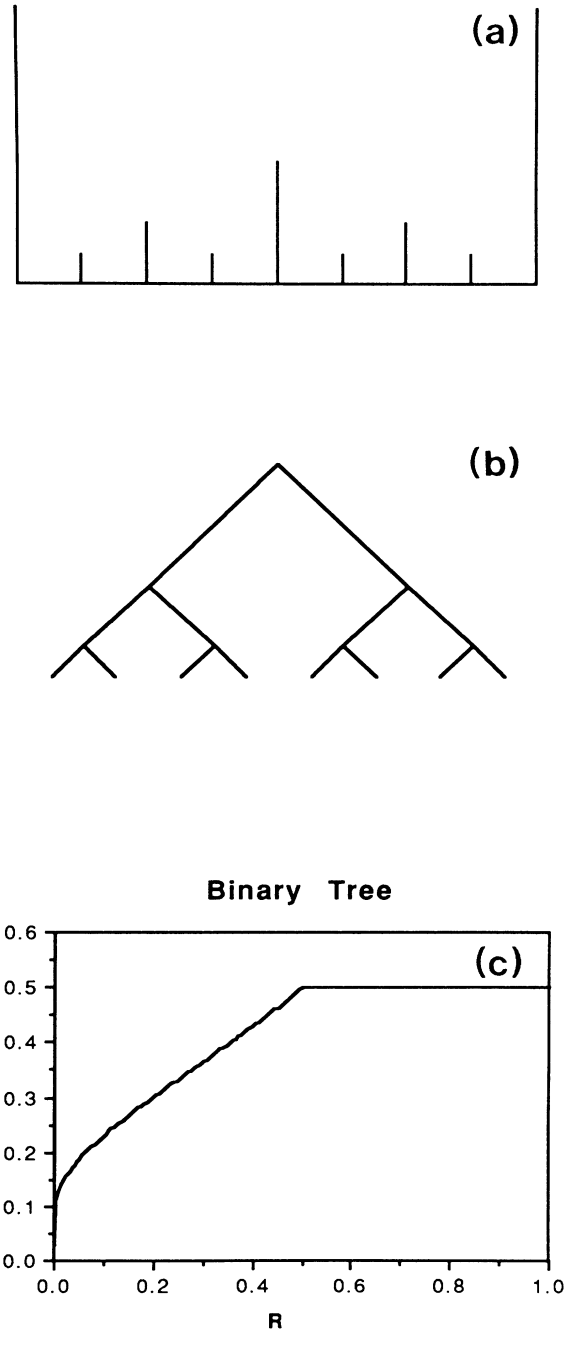

FIG. 1. System with a binary set of barriers (a), represented by an ordered tree, as shown in (b). (c) The exact behavior of the decay exponent ν, as a function of R, for the binary tree.

For the binary system of Fig. 1, the solution for the exponent ν has been found by Huberman and Kerszberg.[4] They gave an approximate solution valid for small values of R and found an anomalous R (and hence temperature) -dependent exponent

$$\nu(R)=\ln(2)/\ln(2/R)\ . \tag{2.3}$$

Teitel and Domany[9] (TD), employing a combination of analytical and numerical methods, found that the HK result holds for R up to $R_c=\frac{1}{2}$; at that point they found a dynamical phase transition to normal diffusion where the exponent $\nu=\frac{1}{2}$ [see Fig. 1(c)]. Maritan and Stella,[10] using renormalization techniques, were the first to give an exact solution of this problem and confirmed the TD result.

As pointed out by Teitel and Domany, the results for the binary case are somewhat more general than may first appear. Zwanzig[11] proves quite generally that for any barrier arrangement, the diffusion constant D is given by

$$\frac{1}{D}=\frac{1}{N}\sum_{n=1}^{N}\frac{1}{\omega_{n,n+1}}\ . \tag{2.4}$$

For the binary tree, this gives $D^{-1}=2/(2R-1)$, and hence the diffusion constant goes to 0 as $R\rightarrow\frac{1}{2}+$. For $R<\frac{1}{2}$, we are in an anomalous regime, in agreement with the exact solution given above. Since this result clearly does not depend on the spatial arrangement of the barriers, one must get the phase transition from normal to anomalous diffusion at $R_c=\frac{1}{2}$ for any rearrangement of the barriers.

Furthermore, if one considers an ensemble of systems which are spatial rearrangements of the barriers in Fig. 1(a), then one may apply the results of Alexander *et al.*[12] on diffusion in random systems to obtain precisely the same results as above. Thus one expects that most rearrangements of the binary tree will behave precisely like

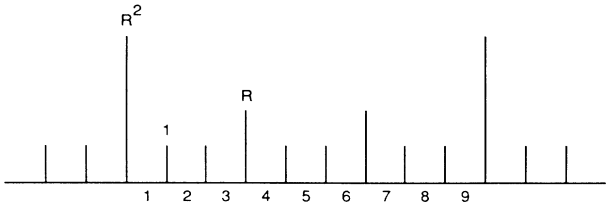

FIG. 2. Portion of the ternary tree.

the ordered case. However, we will see that there exist particular rearrangements which do not yield the same exponent.

III. CURRENT RESULTS

We begin by generalizing the HK method for the binary tree to any regular n-ary tree. For simplicity, we consider the case for $n=3$, but the method will easily carry over for any n. Consider the nine cells shown in Fig. 2, part of a ternary tree with N cells. Letting $\mathbf{P}(t)=(P_1,P_2,\ldots,P_9)$, the master equation gives

$$\frac{d\mathbf{P}}{dt}=-\omega_0\mathsf{A}\mathbf{P}\ , \tag{3.1}$$

where the tridiagonal symmetric matrix A is given by

$$\mathsf{A}=\begin{bmatrix} 1 & -1 & & & & & & & \\ -1 & 2 & -1 & & & & & & \\ & -1 & 1+R & -R & & & & & \\ & & -R & 1+R & -1 & & & & \\ & & & -1 & 2 & -1 & & & \\ & & & & -1 & 1+R & -R & & \\ & & & & & -R & 1+R & -1 & \\ & & & & & & -1 & 2 & -1 \\ & & & & & & & -1 & 1 \end{bmatrix} . \tag{3.2}$$

This result neglects corrections of $O(R^2)$. Integrating gives

$$\mathbf{P}(t)=\exp[-\omega_0\mathsf{A}t]\mathbf{P}(0)\ . \tag{3.3}$$

If we consider times t such that $\omega_0 t \ll 1$, then we may expand the exponential to get

$$\mathbf{P}(t)=(1-\omega_0\mathsf{A}t)\mathbf{P}(0)\ . \tag{3.4}$$

We take the initial state $\mathbf{P}(0)=\frac{1}{3}(1,1,1,0,0,\ldots,0)$. Carrying out the multiplication, we find that

$$\mathbf{P}(t)=\tfrac{1}{3}(1,1,1-R\omega_0 t,R\omega_0 t,0,0,\ldots,0)\ . \tag{3.5}$$

Renormalizing the system by a factor of 3, we have

$$\mathbf{P}'(t)=\left[1-\frac{R\omega_0 t}{3},\frac{R\omega_0 t}{3},0\right] . \tag{3.6}$$

Thus we have a "leakage" across the renormalized second barrier corresponding to a new transition rate $\omega_1'=\omega_1/3$. This renormalization process can be continued, and one finds that each of the transition rates is renormalized to a new value

$$\omega_n'=\omega_n/(3^n)\ . \tag{3.7}$$

Now, following HK, we can write the autocorrelation function in the limit $N\to\infty$ as

$$P_0(t)=2\sum_{n=0}^{\infty}3^{-(n+1)}\exp(-\omega_n' t)\ . \tag{3.8}$$

Note that $P_0(0)=1$. Converting the sum to an integral we get

$$P_0(t)=\tfrac{2}{3}\int_0^{\infty}dn\ 3^{-n}\exp[-(R/3)^n\omega_0 t]\ . \tag{3.9}$$

This integral can be evaluated using a change of variables, with the result that for long times ($\omega_0 t\gg 1$),

$$P_0(t)\approx Ct^{-\nu(R)}\ , \tag{3.10}$$

where

$$\nu(R)=\ln(3)/\ln(3/R)\ , \tag{3.11}$$

$$C=\frac{2}{3}\left[\frac{\Gamma(\nu)}{\ln(3/R)}\right]\omega_0^{-\nu}\ . \tag{3.12}$$

For a general value of n, a similar analysis reproduces Eq. (3.10), with the exponent and prefactor given by

$$\nu(R)=\ln(n)/\ln(n/R)\ , \tag{3.13}$$

$$C=\frac{n-1}{n}\left[\frac{\Gamma(\nu)}{\ln(n/R)}\right]\omega_0^{-\nu}\ . \tag{3.14}$$

These results were derived under the assumption that $R\ll 1$ (we neglected terms of order R^2 in the master equation). If we assume, as is the case for the binary tree, that the analytic form (3.13) holds for all R until $\nu=\frac{1}{2}$, the crossover point to normal diffusion, then we expect a dynamical phase transition at

$$R_c=1/n\ . \tag{3.15}$$

The numerical work we will discuss momentarily strongly supports this conjecture. Furthermore, if we consider the point where the diffusion constant vanishes using Zwanzig's result, we find a transition from normal to anomalous diffusion at precisely the R_c given by (3.13).

IV. COMPUTER EXPERIMENTS

For systems which lack the ordered structure of the binary tree or the regular n-furcating trees, and hence ones for which the renormalization analyses break down, we need to employ numerical methods. We have used

two such methods, one based on explicit diagonalization of the transition matrix in Eq. (2.2), and another based on averages of a large sample of random walks, to analyze several new systems. The mathematical details are given in Appendix A. The diagonalization method directly measures the autocorrelation function $P_0(t)$, and hence determines the exponent $\nu(R)$ from the expected long-time power-law decay $t^{-\nu(R)}$. The random-walk analysis measures the mean squared displacement, which in the long-time limit behaves as $t^{+2\nu(R)}$, and hence yields the same exponent. In the following, we present the results for each of the systems studied, commenting on the important features found in each case.

A. Binary tree [Fig. 3(a)]

We begin by testing the numerical methods on a tree where we have an exact solution. In Fig. 3(b), we have plotted the measured exponent $\nu(R)$ versus R. The solid curve represents the theoretical solution given by Eq. (2.3), with the phase transition to normal diffusion at $R=\frac{1}{2}$. The R dependence of the exponent for $R<R_c$ is apparent; the singularity at R_c is somewhat diffuse, but crossover to normal diffusion at large R is clear. The agreement of the numerical data with the theoretical predictions is typically to within about 5%.

B. Ternary tree [Fig. 4(a)]

Figure 4(b) presents the measured exponent for the ternary tree. This is the first case where we observe the dynamical phase transition at a point other than $\frac{1}{2}$.

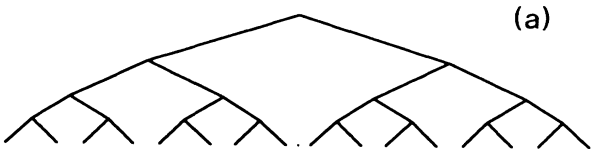

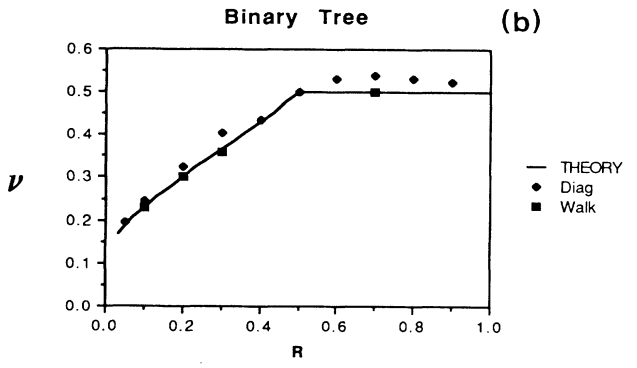

FIG. 3. Observed behavior of the relaxation exponent for the binary tree shown in (a). (b) The solid line denotes the theoretical prediction, the dots correspond to numerical matrix diagonalization, and the squares are the results of random-walk simulations. Statistical errors, here and in the following graphs, are of the order of the size of the dots, or smaller.

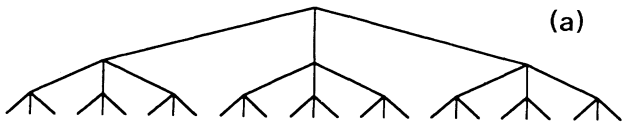

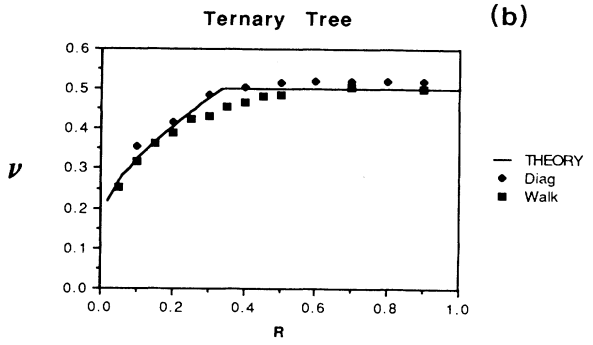

FIG. 4. Observed behavior of the relaxation exponent for the ternary tree shown in (a). (b) The solid line denotes the theoretical prediction, the dots correspond to numerical matrix diagonalization, and the squares are the results of random-walk simulations.

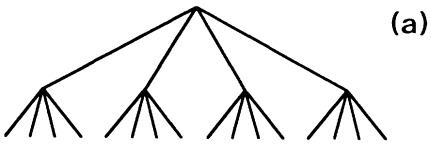

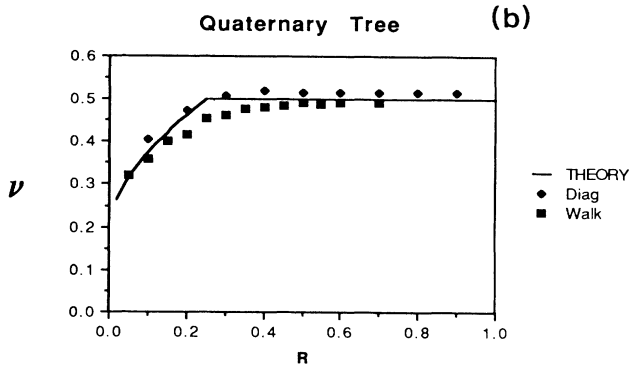

FIG. 5. Observed behavior of the relaxation exponent for the quaternary tree shown in (a). (b) The solid line denotes the theoretical prediction, the dots correspond to numerical matrix diagonalization, and the squares are the results of random-walk simulations.

C. Quaternary tree [Fig. 5(a)]

The ordered quaternary tree allows us to check the generalized predictions of Eq. (3.13). The solid line represents the theoretical prediction, and again the agreement with experiment is quite good.

D. Fibonacci tree [Fig. 6(a)]

The "Fibonacci" tree of Fig. 6(a) is an example of a "random" tree—i.e., one in which the branching ratio is nonconstant, even on a local scale. The tree is generated by the following algorithm. At the root there is one parent node. The next generation includes the parent, and a single offspring. From then on, any offspring must wait one generation before it becomes a parent; parents, meanwhile, reproduce at every generation. There are no deaths. Thus if tree produced has a population f_n at the nth generation, then

$$f_n = f_{n-1} + f_{n-2} \quad \text{for } n \geq 2 \text{ with } f_0 = f_1 = 1 \ . \tag{4.1}$$

Clearly, the series $\{f_n\}$ is just the famous Fibonacci sequence (hence the name of the tree).

If one now treats this tree as random, then the results of Alexander *et al.* can be applied. They find that for a system of barriers with a density of transition rates $\rho(\omega) \approx \omega^{-\alpha}$ as $\omega \to 0$, that the autocorrelation function behaves, in the limit $t \to \infty$, as

$$P_0(t) \approx \begin{cases} t^{-(1-\alpha)/(2-\alpha)}, & \alpha > 0 \\ t^{-1/2}, & \alpha < 0 \ . \end{cases} \tag{4.2}$$

In our case, we have $\alpha = 1 + \ln(g)/\ln(R)$, where $g = (\sqrt{5}+1)/2$ is the golden mean. Inserting this expression into Eq. (4.2) gives

$$P_0(t) \approx \begin{cases} t^{-\ln(g)/\ln(g/R)}, & R < 1/g \\ t^{-1/2}, & R > 1/g \ . \end{cases} \tag{4.3}$$

Thus we predict a dynamical phase transition between normal and anomalous diffusion at $R_c = 1/g \approx 0.618$.

In Fig. 6(b), we have plotted the results of the numerical measurements of the exponent. We see that the agreement with the prediction of Eq. (4.3) is excellent.

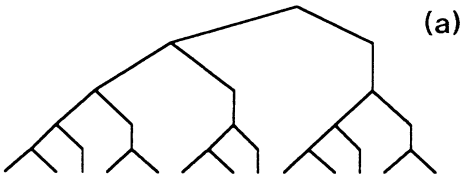

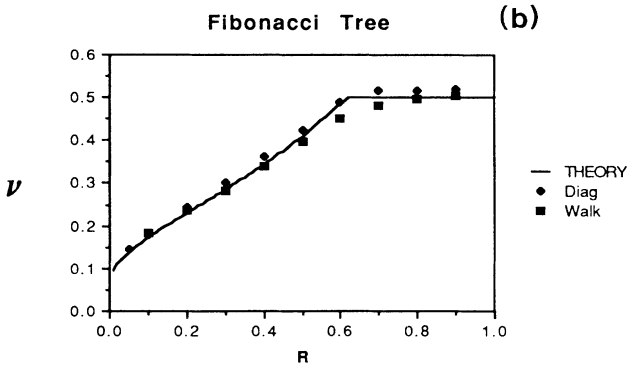

FIG. 6. Observed behavior of the relaxation exponent for the Fibonacci tree shown in (a). (b) The solid line denotes the theoretical prediction, the dots correspond to numerical matrix diagonalization, and the squares are the results of random-walk simulations.

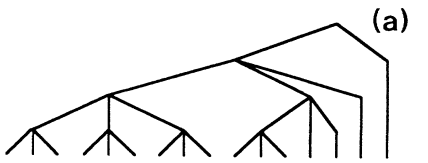

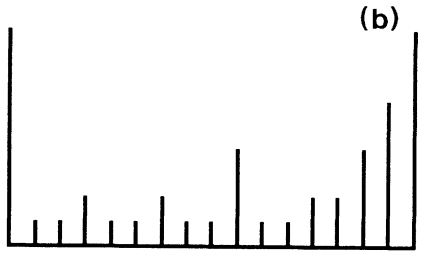

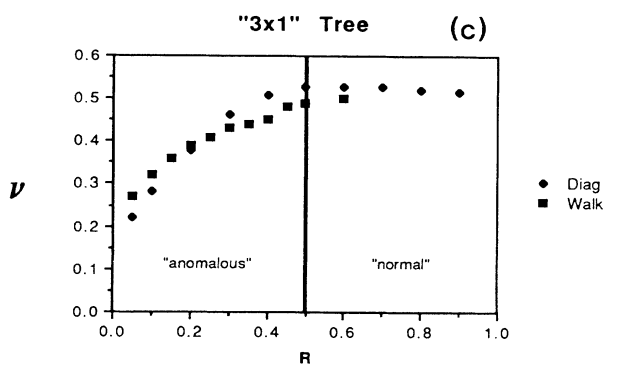

FIG. 7. (a) Most diverse tree ("3×1") representing the complex barrier arrangement shown in (b). (c) The measured exponent as a function of R. The dots correspond to numerical matrix diagonalization and the squares are the results of random-walk simulations.

E. "3×1" tree [Fig. 7(a)]

The next system we study corresponds to a tree intermediate between ordered and random—i.e., a "complex" tree in the terminology of Huberman and Hogg[13] [Fig. 7(a)]. It was introduced in the study of long-range hopping processes by Bachas and Huberman,[6] who proved that it produces the slowest rate of decay possible. At any generation, the left one-half members trifurcate and the right one-half members have a single offspring. The significance of this tree to the nearest-neighbor hopping problem comes from the fact that the barriers are precisely the same as those in the binary-tree system (Sec. IV A), just arranged in a different spatial order [Fig. 7(b)]. Considering the fact that random rearrangements of the binary tree yield the same exponent as the ordered case led TD to conjecture[8,9] that any particular rearrangement will lead to the same results, as well.

However, as Fig. 7(c) shows, this particular rearrangement appears to have a different form for the exponent for $R < \frac{1}{2}$. The dynamical phase transition still occurs at $R_c = \frac{1}{2}$, as required by the general results of Zwanzig. Furthermore, for small values of R, the exponent agrees quite closely with that of the ordered ternary tree (Sec. IV B). As R approaches $\frac{1}{2}$, however, the exponent slowly crosses over to the ordered binary case. Thus in some sense, this tree is intermediate between the binary and ternary tree. Unfortunately, no analytical explanation of these results for the 3×1 tree exists at present.

F. "5×1" tree [Fig. 8(a)]

The "5×1" tree is another rearrangement of the barriers found in the ordered binary case. To construct this tree, let the leftmost one-quarter nodes pentafurcate and the rightmost three-quarters have single offspring at each generation [see Fig. 8(a)]. From the plot in Fig. 8(b), we see that again we have the required transition at $R_c = \frac{1}{2}$, but that the exponent for $R < R_c$ differs from the binary case. In fact, for R very small, it agrees quite closely with the result for an ordered quinary tree. As R increases towards one-half, the exponent continuously crosses over to the binary case, just as in the 3×1 tree above.

V. HIGHER-DIMENSIONAL RESULTS

One can generalize the argument of Sec. III to include systems of higher dimensions.[14] We only consider d-dimensional cases that are "direct products" of d ordered one-dimensional systems. Figure 9(a) shows a two-dimensional case that is the direct product of two 1D binary systems [Fig. 1(a)]. Let us examine this case, as the generalization to an arbitrary d-dimensional system that is the cross product of d 1D ordered n-ary systems is straightforward.

The analysis in Sec. III up to Eq. (3.4) holds, except that the matrix A changes. The initial state, which we

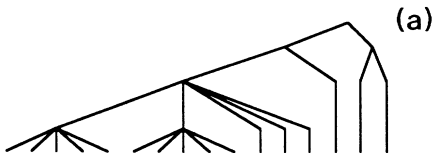

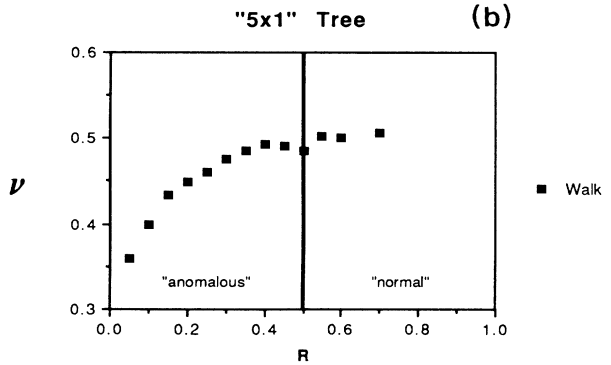

FIG. 8. (a) "5×1" tree and (b) the measured exponent as a function of R. The dots correspond to numerical matrix diagonalization and the squares are the results of random-walk simulations.

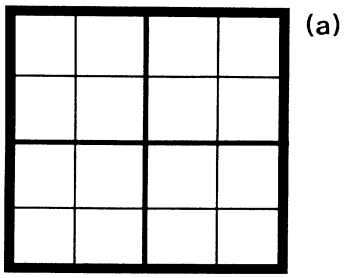

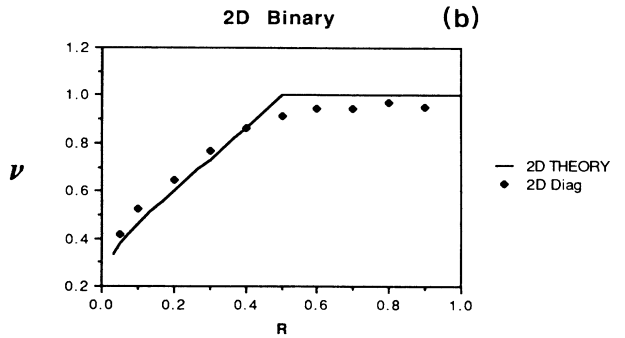

FIG. 9. (a) Square grid representing a two-dimensional hierarchical system. (b) The measured exponent as a function of R. The dots correspond to numerical matrix diagonalization and the squares are the results of random-walk simulations.

write in a matrix form similar to the layout of the cells themselves in Fig. 9(a), is given by

$$\mathsf{P}(0)=\tfrac{1}{4}\begin{bmatrix}1&1&0&0\\1&1&0&0\\0&0&0&0\\0&0&0&0\end{bmatrix}. \tag{5.1}$$

The state of the system at a short time t later ($\omega_0 t \ll 1$) is

$$\mathsf{P}(t)=\tfrac{1}{4}\begin{bmatrix}1&1-R\omega_0 t&R\omega_0 t&0\\1-R\omega_0 t&1-2R\omega_0 t&R\omega_0 t&0\\R\omega_0 t&R\omega_0 t&0&0\\0&0&0&0\end{bmatrix}. \tag{5.2}$$

Thus in a renormalized picture it is as if $\mathsf{P}(t)\rightarrow\mathsf{P}'(t)$ were given by

$$\mathsf{P}(t)=\begin{bmatrix}1-R\omega_0 t&\frac{1}{2}R\omega_0 t\\\frac{1}{2}R\omega_0 t&0\end{bmatrix}. \tag{5.3}$$

Hence, we can identify a renormalized transition rate $\omega_1'=\omega_1/2=R\omega_0/2$. This renormalization procedure can be repeated and we find that ω_n will be renormalized to $\omega_k'=\omega_k/(2^k)$, just as in the one-dimensional case. The autocorrelation function is now given by

$$P_0(t)=3\sum_{k=0}^{\infty}(2^2)^{-k}\exp(-\omega_k' t)$$
$$\rightarrow 3\int_0^{\infty} dk\, 4^{-k}\exp[-(R/2)^k\omega_0 t]\,. \tag{5.4}$$

Evaluation of this integral in the long-time limit ($\omega_0 t \gg 1$), as in Sec. III, leads to $P_0(t)\approx t^{-\nu}$, where

$$\nu_{2D}(R)=2\ln(2)/\ln(2/R)=2\nu_{1D}\ \text{(2D binary case)}\,. \tag{5.5}$$

In d dimensions, the above result changes only in that the renormalization procedure involves 2^d cells, instead of 2 (for 1D) or 4 (for 2D). If one considers an ordered n-ary tree instead of the binary tree described above, then the only difference is that $\omega_k'=\omega_k/(n^k)$, and that one renormalizes over n^d cells. Thus the autocorrelation function is given by

$$P_0(t)=(n^d-1)\sum_{k=0}^{\infty}(n^d)^{-k}\exp(-\omega_k' t)\,, \tag{5.6}$$

and the long-time behavior is governed by the exponent

$$\nu_{dD}(n,R)=d\ln(n)/\ln(n/R)=d\nu_{1D}$$
$$\text{(general case)}\,. \tag{5.7}$$

Although these results were all derived in the limit of small R, one might guess that they may hold until $\nu=d/2$, which is the exponent for normal diffusion in d dimensions. If so, this would imply a dynamical phase transition at $R_c=1/n$, just as in the one-dimensional case.

We have numerically investigated the 2D binary case using the eigenvalue method. Numerical considerations limited us to systems of about $16^2=256$ cells. The results, given in Fig. 9(b), are consistent with the prediction of Eq. (5.5), along with the conjectured phase transition at $R_c=\frac{1}{2}$. However, because of the small system size and the lack of precision in the experiment, we can claim no definite proof of the above.

VI. SUMMARY

In this paper, we have studied the phenomenon of ultradiffusion in arbitrary trees with nearest-neighbor hoppings. We have found universality in the qualitative features of ultradiffusion: an anomalous R-dependent exponent for $R<R_c$, and a singular crossover at R_c to normal diffusion. Moreover, the value of R_c depends on the average branching ratio of the system. Furthermore, we discovered a set of trees, for which the R dependence of the exponent departs from the expected value based on universality arguments.

Since nearest-neighbor hopping processes sample a fairly local region of ultrametric space, it is not clear at present to what extent these newly found anomalies depend on the overall complexity of a given tree. As the simulations are constrained to operate between a time scale containing no transients and an upper bound determined by computer limitations, the extent to which the entire tree is sampled during a given experiment is small. Thus, unlike the case of arbitrary range hopping solved by Bachas and Huberman, these processes do not convey much information on the complexity of the barrier distributions. They nevertheless apply to very general hierarchical situations and exhibit dynamical singularities which should be observable in experiments measuring the decay of the autocorrelation function in physical systems.

ACKNOWLEDGMENTS

We have benefited from discussions with Constantin Bachas and Wilfried Wolff. We thank S. Teitel and E. Domany for sending us results of their work prior to publication. This work was partially supported by U.S. Naval Research Laboratory (ONR) Contract No. N0001-14-82-0699.

APPENDIX

In this appendix, we give the details of the two numerical procedures used in Secs. IV and V. First, let us describe the diagonalization method. One begins with the master equation (2.2). We can rewrite this as

$$\frac{d\mathbf{P}}{dt}=-\Omega\mathbf{P}\,, \tag{A1}$$

where the matrix Ω is given by

$$\Omega_{ij}=\begin{cases}\omega_{i-1;i}+\omega_{i;i+1}, & i=j\\-\omega_{i-1;i}, & i=j+1\\-\omega_{i;i+1}, & i=j-1\\0, & \text{otherwise}\,.\end{cases} \tag{A2}$$

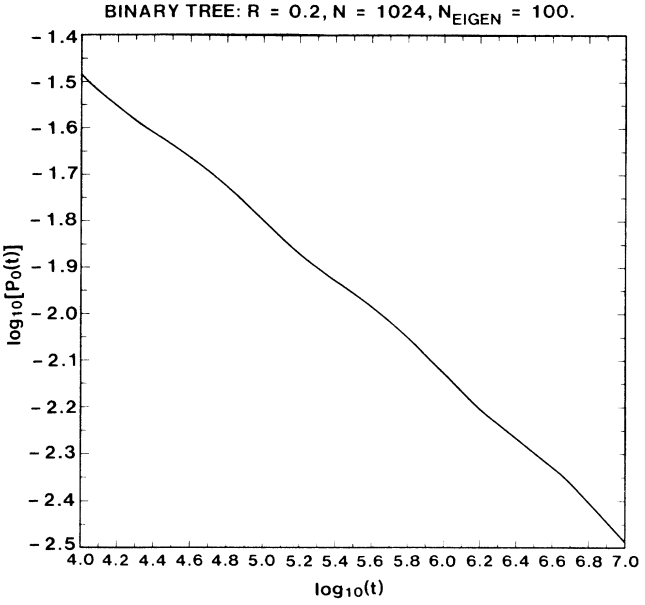

FIG. 10. Typical plot of the $\log_{10}[P_0(t)]$ vs $\log_{10}(t)$, for the diagonalization method. The best-fit slope gives the exponent.

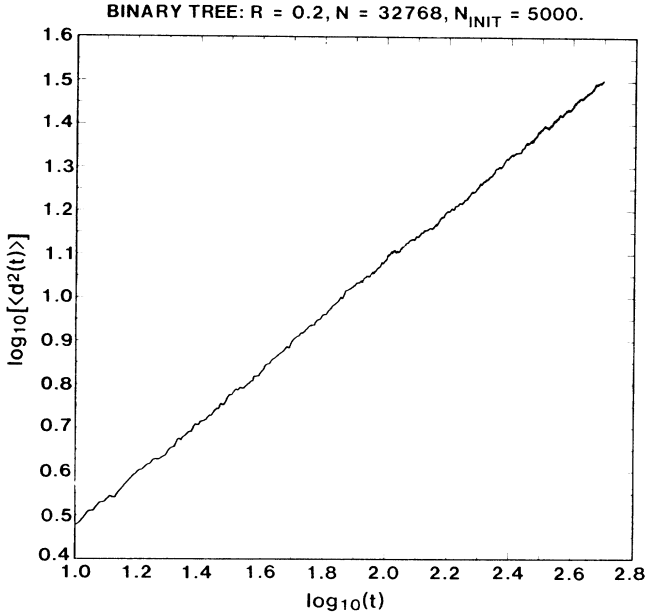

FIG. 11. Typical plot of $\log_{10}\langle d^2(t)\rangle$ vs $\log_{10}(t)$ for a random-walk simulation. The slope gives the exponent for the mean-square displacement.

We assume here that we have a system of N cells labeled from 1 to N, and that the basic unit of time is determined by requiring $\omega_0=1$. Then, $\omega_n=R^n$. Furthermore, we take the boundary conditions to be $\omega_{0,1}=\omega_{N,N+1}=0$. Clearly, Ω is a symmetric matrix, and hence can be diagonalized. Letting Λ be the diagonal matrix containing the eigenvalues $\{\lambda_j\}$ of Ω and S be the corresponding matrix of eigenvectors $\{\mathbf{x}_j\}$ which diagonalizes Ω, then we have

$$\mathbf{P}(t)=[\mathrm{S}\exp(-\Lambda t)\mathrm{S}^T]\mathbf{P}(0)\ . \tag{A3}$$

If we assume $P_n(0)=\delta_{n,0}$, then $P_0(t)$ is given by

$$P_0(t)=\sum_j \exp(-\lambda_j t)(\mathbf{x}_j)_0^2\ . \tag{A4}$$

The sum is over all the cells j in the system. We now average over all initial states in the system. Then, because each of the eigenvectors $\mathbf{x}_j$ is normalized, we find that the average autocorrelation function is

$$\langle P_0(t)\rangle=\frac{1}{N}\sum_{j=1}^{N}\exp(-\lambda_j t)\ . \tag{A5}$$

Because the matrix Ω is tridiagonal, there exist efficient routines to find the eigenvalues. Since we are interested in the long-time limit of $P_0(t)$, only the smallest eigenvalues of Ω are needed. Typically, we examined systems of size $N\approx 1000$, and found the smallest 100 eigenvalues. The sum in (A5) was evaluated and plotted on a log-log plot. The exponent ν was determined from the slope of the best-fit line to the data. Increasing the number of eigenvalues found did not appreciably improve the results. Increasing the system size by an order of magnitude did improve the precision, but at a cost of considerable computer time.

One should note that as $t\to\infty$, the limit of (A5) gives an exponential decay of the autocorrelation function. However, for large N, enough eigenvalues cluster near zero to give an algebraic decay for long, but not too long, times. An example of the typical long-time behavior of $\log_{10}[P_0(t)]$ versus $\log_{10}(t)$ is given in Fig. 10. Notice that the slope is somewhat steeper at large values of t.

Next, let us describe the random-walk method for measuring the mean-square displacement (MSD). Again one considers a system of N cells, with the master equation and boundary conditions being the same as above. This time we simulate actual particle motion according to the following rules.

At $t=0$, we randomly place the particle in one of the cells, call it n. At time $t=\tau$, a random number r between 0 and 1 is generated. If $\omega_{n,n-1}\tau<r$, then the particle hops to the left; if $(1-r)<\omega_{n,n+1}\tau<1$, then the particle hops to the right; otherwise, the particle remains in cell n at the next time step. Clearly, we must have $(\omega_{n,n-1}+\omega_{n,n+1})\tau\le 1$; since $\omega_{i,j}\le 1$, we see that the largest time step we may pick in general is $\tau=\frac{1}{2}$. To make the simulation as fast as possible, we used this maximum value for τ.

The above process is repeated at every time step $t_k=k\tau$. At each step, we keep track of the squared distance from the starting cell n. The process was carried out for some large number of steps, typically 1000 or 10 000. To obtain the mean-square displacement (MSD), we repeated the experiment numerous times, starting each case at a new randomly selected position. We typically averaged over 5000 initial points for a system of size $N\approx 30\,000$. The MSD was then plotted vs. time on a log-log plot, and the slope was measured. A typical example of such a plot is given in Fig. 11.

[1]H. Simon, *The Sciences of the Artificial* (MIT, Cambridge, Mass., 1962).

[2]See, for example, A. Ansari, J. Benendzen, S. Browne, H. Frauenfelder, I. Iben, T. Sauke, E. Shyamsunder, and R. Young, Proc. Natl. Acad. Sci. U.S.A. **82**, 5000 (1982).

[3]M. Mézard, G. Parisi, N. Sourlas, G. Toulouse, and M. Virasoro, Phys. Rev. Lett. **52**, 1156 (1984); J. Phys. (Paris) **45**, 843 (1984).

[4]B. A. Huberman and M. Kerszberg, J. Phys. A **18**, L331 (1985).

[5]See, for example, M. Schreckenberg, Z. Phys. B **60**, 483 (1985); A. T. Ogielski and D. L. Stein, Phys. Rev. Lett. **55**, 1634 (1985); G. Paladin, M. Mézard, and C. de Dominicis, J. Phys. (Paris) Lett. **46**, L985 (1985); Z. Qiang, Acad. Sinica (to be published).

[6]C. Bachas and B. A. Huberman, Phys. Rev. Lett. **57**, 1965 (1986).

[7]J. Meiss and E. Ott, Phys. Rev. Lett. **55**, 2741 (1986); Physica **20D**, 387 (1986); S. Grossmann, F. Wegner, and K. Hoffmann, J. Phys. (Paris) Lett. **46**, L575 (1985).

[8]S. Teitel, D. Kutasov, and E. Domany, Phys. Rev. B **36**, 684 (1987).

[9]S. Teitel and E. Domany, Phys. Rev. Lett. **55**, 2176 (1985).

[10]A. Maritan and A. L. Stella, Phys. Rev. Lett. **56**, 1754 (1986); J. Phys. A **19**, L269 (1986).

[11]R. Zwanzig, J. Stat. Phys. **28**, 127 (1982).

[12]S. Alexander, J. Bernasconi, W. R. Schneider, and R. Orbach, Rev. Mod. Phys. **53**, 175 (1981).

[13]B. A. Huberman and T. Hogg, Physica **22D**, 376 (1986).

[14]H. A. Ceccato and J. A. Riera, J. Phys. A **19**, L721 (1986).